Article

The Melon *Zym* Locus Conferring Resistance to ZYMV: High Resolution Mapping and Candidate Gene Identification

Nastacia Adler-Berke [1,†], Yitzchak Goldenberg [1,†], Yariv Brotman [1,2], Irina Kovalski [1], Amit Gal-On [3], Tirza Doniger [1], Rotem Harel-Beja [4], Christelle Troadec [5], Abdelhafid Bendahmane [5], Michel Pitrat [6], Catherine Dogimont [6], Nurit Katzir [4] and Rafael Perl-Treves [1,*]

1   Faculty of Life Sciences, Bar-Ilan University, Ramat Gan 5290002, Israel; nastaciast@gmail.com (N.A.-B.); gimzo2000@gmail.com (Y.G.); brotmany@post.bgu.ac.il (Y.B.); irinak49@gmail.com (I.K.); tirza.doniger@gmail.com (T.D.)
2   Department of Life Sciences, Ben-Gurion University of the Negev, Beersheba 8410501, Israel
3   Department of Virology, Agricultural Research Organization, Rishon LeZion 7505101, Israel; amitg@volcani.agri.gov.il
4   Newe Yaar Research Centre, Agricultural Research Organization, Ramat Yishay 30095, Israel; rotemhb@volcani.agri.gov.il (R.H.-B.); nurit.katzir@gmail.com (N.K.)
5   Institute of Plant Sciences, Université Paris-Saclay, 91190 Gif-sur-Yvette, France; christelle.troadec@inrae.fr (C.T.); abdelhafid.bendahmane@inra.fr (A.B.)
6   Unite de Génétique et Amélioration des Fruits et Légumes, INRA, 84143 Montfavet, France; michelpitrat@orange.fr (M.P.); catherine.dogimont@inrae.fr (C.D.)
*   Correspondence: rafi.perl@gmail.com
†   Equal contribution.

Abstract: Zucchini yellow mosaic virus (ZYMV; *potyviridae*) represents a major pathogen of *Cucurbitaceae* crops. ZYMV resistance in melon PI 414723 is conditioned by a dominant allele at the *Zym* locus. This resistant accession restricts viral spread and does not develop mosaic symptoms, but necrosis sometimes develops in response to inoculation. In previous studies, *Zym* has been mapped to linkage group II of the melon genetic map. In the present study, positional cloning of the locus was undertaken, starting from the CM-AG36 SSR marker at approximately 2 cm distance. We utilized five mapping populations that share the same resistant parent, PI 414723, and analyzed a total of 1630 offspring, to construct a high-resolution genetic map of the *Zym* locus. Two melon BAC libraries were used for chromosome walking and for developing new markers closer to the resistance gene by BAC-end sequencing. A BAC contig was constructed, and we identified a single BAC clone, from the ZYMV susceptible genotype MR-1, that physically encompasses the resistance gene. A second clone was isolated from another susceptible genotype, WMR 29, and the two clones were fully sequenced and annotated. Additional markers derived from the sequenced region delimited the region to 17.6 kb of a sequence that harbors a NAC-like transcription factor and, depending on the genotype, either two or three *R*-gene homologs with a CC-NBS-LRR structure. Mapping was confirmed by saturating the map with SNP markers using a single mapping population. The same region was amplified and sequenced also in the ZYMV resistant genotype PI 414723. Because numerous polymorphic sites were noted between genotypes, we could not associate resistance with a specific DNA polymorphism; however, this study enables molecular identification of *Zym* and paves the way to functional studies of this important locus.

Keywords: *Cucumis melo*; melon; zucchini yellow mosaic virus; ZYMV; resistance gene; DNA markers; positional cloning; NBS-LRR

1. Introduction

Melon (*Cucumis melo* L.) is an economically important diploid species of the *Cucurbitaceae* family. It has 12 chromosomes (2n = 2x = 24) and an estimated genome size of 450 to 500 Mbp [1]. A fist genomic sequence of a melon dihaploid breeding line, DHL92,

was published by Garcia-Mas et al. in 2012 [2] and rendered available in the Cucurbit Genomics Database (http://cucurbitgenomics.org/, assembly # GCA_000313045.1). Recently, Castanera et al. [3] employed third generation sequencing methods that read long DNA molecules (PacBio) to fill remaining gaps and produce a refined version of the DHL92 genome and its annotation, deposited in the Melonomics Database (GCA_902497455.1; https://www.melonomics.net/melonomics.html). Yano et al. [4] used the Oxford nanopore technology and sequenced a Japanese *var. reticulatus* variety, Harukei-3 (GCA_011762645.1), along with extensive expression data in vegetative and reproductive melon tissues, deposited in the Melonet-DB gene expression atlas [5]. The genome of a Chinese variety, Paizawat (a sweet, thick-skinned spp. *melo* variety) was assembled by Zhang et al. [6] using Pac-Bio long molecule sequencing, combined with the Hi-C interaction analysis to verify the accuracy of assembly. Finally, using a similar methodology, Yang et al. [7] turned to sequence an accession of the *Cucumis melo subspecies agrestis*, *var conomon*, that has been less well studied, focusing on gummy stem blight resistance and sugar accumulation traits. More genomes of Korean varieties (var. Makuwa of the *Conomon* group) have been assembled to the scaffold level and deposited in the GenBank (GCA_005549215.1, GCA_005549225.1). In the re-sequencing era, attention has shifted to genome polymorphism and evolution, and more assemblies are expected.

Genes conferring resistance against diverse melon pathogens and pests have been identified in "exotic" melon accessions, and mapped using different mapping populations [8–12]. Later, highly saturated maps have been produced, linking genetic maps from different populations with the draft genome by Garcia-Mas et al. and enabling the localization of QTL and single genes (e.g., review by [13]). The development of full genomic and transcriptomic sequences and new mapping approaches, such as genotyping by sequencing (GBS), and availability of core collections and Introgression Lines, produced a plethora of mapping studies (e.g., [14,15] and references therein). For example, Wang et al. [16] mapped at high resolution downy mildew resistance in melon and identified a likely candidate, a receptor kinase gene; Giner et al. [17] mapped CMV resistance, and we have finely mapped PRSV and Fusarium resistances [18].

Zucchini yellow mosaic virus (ZYMV) is a member of the *potyviridae* family, the largest family of plant viruses [19]. ZYMV is transmitted non-persistently by a number of aphid species and represents a major pathogen of *Cucurbitaceae* crops, causing severe yield losses and quality defects [20,21]. The ZYMV genome consists of a single messenger-polarity RNA molecule of about 10 kb, encapsidated in a flexuous filamentous particle. Viral RNA is translated into a large polyprotein that is proteolytically processed to 11 functional proteins by three virus-encoded proteases: P1, HC-Pro and NIa [22,23]. Over the years, full sequences of numerous ZYMV isolates from different geographic regions have been published [24–26], contributing to understanding ZYMV epidemiology and evolution. Moreover, knowledge on ZYMV infectivity and plant defense responses against ZYMV has expanded notably, e.g., [27,28].

The Indian melon plant introduction PI 414723 [29] is the only genetically characterized source for ZYMV resistance in melon. When crossed with susceptible cultivars such as 'Védrantais', ZYMV resistance is inherited as a single dominant gene designated *Zym* [30]. Resistant progeny may either remain symptomless, or, due to poorly understood environmental or genetic interactions, react to ZYMV by developing necrosis of leaves and stems that, in extreme cases, could cause stunting or even death of the plant. In addition to genetic resistance, transgenic and cross-protection strategies have been developed for the control of ZYMV [31–33].

The *Zym* gene has been mapped to the linkage group II of the melon genetic map using a 159-progeny population from the cross between the line PI 414723 and Dulce, and an SSR marker, CMAG36, linked at a 2 cm distance from *Zym* has been identified [34]. In the present study, two melon BAC libraries, both from susceptible genotypes, were used for chromosome walking and physical mapping of the *Zym* locus. High resolution mapping relied on progeny from five mapping populations, prepared by crossing resistant PI 414723

with different ZYMV-susceptible genotypes. Several new SNP markers closer to the gene have been developed based on BAC sequences, and screened across the five mapping populations, comprising 1630 progeny in total, along with ZYMV inoculation. This led to the sequencing of the region in susceptible and resistant genotypes and the identification of gene-candidates for *Zym*. As a second approach to mapping, one of the populations was saturated with SNP markers obtained by RNAseq profiling of 79 RIL progeny [35,36], and the respective ZYMV resistance scores were subjected to QTL analysis, leading to independent identification of the same chromosomal region.

2. Materials and Methods

2.1. Mapping Populations and Overall Experimental Design

Five mapping populations were utilized for mapping of the *Zym* locus. Table 1 specifies the crosses used to generate each population, population size, and reference to the literature. Mapping involved two stages, as evidenced in the Section 3. Initial mapping involved three recombinant inbred line (RIL) populations, namely Populations 1–3, where all the respective progeny underwent ZYMV inoculation tests and genotyping with markers. Chromosome walking on a melon BAC library started from a distant marker, CM-AG36. Parallel to chromosome walking and construction of a BAC contig, populations 1–3 were scored with markers that we developed from BAC end sequences. This resulted in a medium-resolution genetic map that was anchored to the BAC contig, and culminated in the isolation of a single BAC clone encompassing the *Zym* locus. Populations 4–5 were an F_2 and a BC_1 population, respectively, that were added to increase mapping resolution: in these two populations, only individuals displaying recombination around the locus were inoculated with ZYMV. ZYMV inoculation (see below) was performed on the progeny, i.e., F_3 and BC_1-S_1 families derived by self-pollination of F_2 and BC_1 individuals from populations 4 and 5, respectively. The polymorphic markers used to achieve the higher resolution map and to define the smallest physical interval for *Zym* were developed after sequencing the entire BAC and searching for SNP among the parents of the different populations.

Table 1. Five melon populations used in this study to map the *Zym* locus at high resolution. Population type, parental genotypes, bibliographic reference, and numbers of progeny are shown. In populations 4 and 5, DNA genotyping was done in the F_2 and BC_1 generations, while ZYMV inoculation was performed on samples of the individuals' F_2-F_3 and BC_1-S_1 progeny, respectively.

Population Number	Type	ZYMV-Resistant Parent	ZYMV-Susceptible Parent	Reference	# Offspring
1	RIL	PI 414723	Dulce	Harel-Beja et al., 2010	97
2	RIL	PI 414723	Top Mark	This study	103
3	RIL	PI 414723	Védrantais	Périn et al., 2002	61
4	F_2	PI 414723	BIZ	Herman & Perl-Treves, 2007 [37]	141
5	BC_1	PI 414723	Védrantais	Brotman et al., 2013	1228

2.2. Scoring for ZYMV Resistance

Inoculation of Populations 1 and 3 was reported by [8,35], respectively. In the present study, Populations 2, 4, and 5 were scored. A non-aphid-transmissible ZYMV isolate (ZYMV-AG) was provided by Dr. A. Gal-On, ARO. Twenty-five progeny of each RIL, BC_1-S_1 or F_2-F_3 family, respectively, along with parental lines as a control, were grown in a growth chamber (16:8 h light: dark cycle, 25 °C), using 5 plants per 250 mL pot. At the emergence of the first true leaf, melon seedlings were inoculated by rubbing the cotyledons and true leaf with an infective homogenate prepared from 1 g of susceptible zucchini leaves at 14 dpi, diluted in 5 mL water, with carborundum abrasive powder.

Plants were visually scored as resistant or susceptible at 14 and 21 dpi, compared to the response of the parental lines in each trial. Plants were classified as resistant if they were symptomless or had systemic chlorotic or necrotic spots on their stems and leaves, as in PI 414723. Individual plants were classified susceptible if they had mosaic symptoms (that could be accompanied with leaf distortion and stunting). Figure 1A exemplifies the ZYMV resistance and susceptibility phenotypes. RIL lines were designated as homozygous resistant or homozygous susceptible; F_3 and BC-S_1 families were either segregating or uniform, enabling the designation of the parental BC_1 or F_2 plants as either homozygous-resistant (*Zym/Zym*), homozygous susceptible (*zym/zym*), or heterozygous (*Zym/zym*). Individuals that had a cross-over event in the *Zym* region, as well as cases where genotype designation was ambiguous, were scored at least twice.
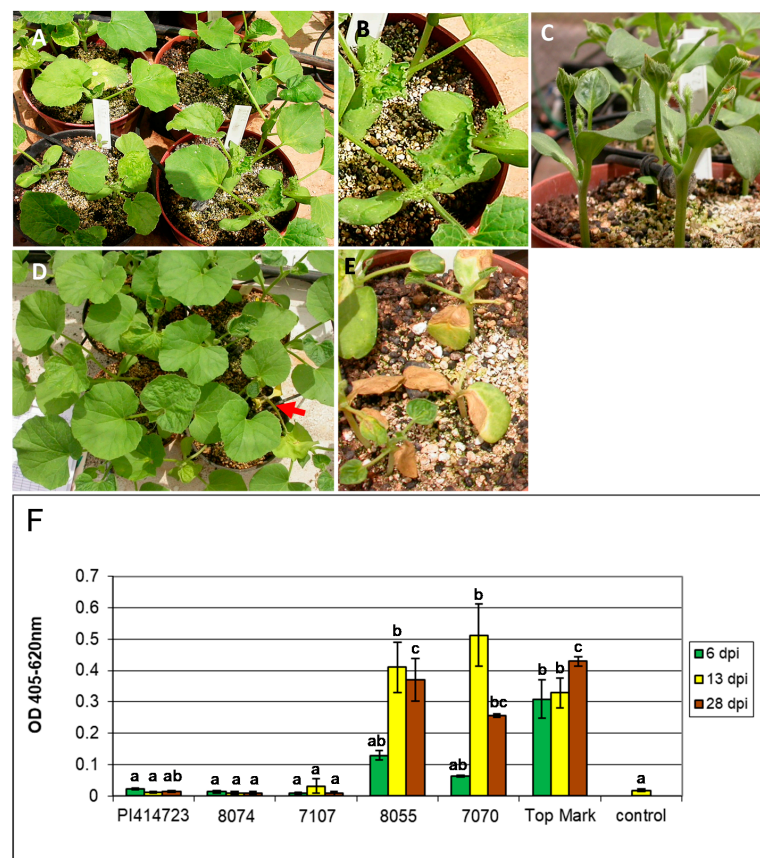
Figure 1. Phenotype and virus titer of ZYMV inoculated melon plants. (**A**–**E**). ZYMV symptoms 21 days after hand-inoculation of representative Population 3 RIL families with ZYMV-inoculated leaf extracts. (**A**)—susceptible RIL family showing mosaic symptoms and some growth retardation. (**B**)—close up of above plants. (**C**)—susceptible family with dwarfing symptoms and no necrosis. (**D**)—resistant family, most plants symptomless with full growth. Arrow points at a plant with petiole necrosis. (**E**)—In certain ZYMV resistant families, mostly under hot temperature, necrosis can become extreme. (**F**) Spread of ZYMV in melon plants is effectively restricted by the *Zym* gene. The Double-antibody ELISA sandwich assay was performed using a polyclonal antibody raised against the ZYMV coat protein. Average absorbance at 405 nm was plotted (n = 3 biological replicates) at 6, 13, and 28 dpi. Two-way ANOVA followed by Tukey post-hoc test comparing genotypes separately for each of the three sampling dates shows significant differences at $p < 0.05$ (marked by different letters) between nearly every resistant/susceptible genotype comparison. Differences between sampling dates of each genotype were insignificant. Non inoculated control plants were sampled for ELISA at 13 dpi. They did not develop any symptoms and their virus titer values were practically below detection and did not differ from inoculated resistant genotypes (1-way ANOVA, Dunnet post hoc test).

ZYMV titer was measured using a double antibody sandwich ELISA (enzyme linked immunosorbent assay; Clark and Adams [38]). Ninety-six well ELISA plates, pre-coated with rabbit polyclonal antibody raised against purified ZYMV coat protein, diluted 1:2000 in coating buffer (15 mM Na_2CO_3, 35 mM $NaHCO_3$, 3 mM NaN_3, pH = 9.6). After overnight incubation at 4 °C, plates were washed six times in PBS-T (80 g NaCl, 0.2 g KCl, 2.9 g $Na_2HPO_4 \cdot 12H_2O$, 0.5 mL Tween 20 in 1 L, pH = 7.4 adjusted with HCl) and dried. Two leaf discs (5 mm) were collected from each plant, homogenized in 0.5 mL homogenization buffer (3 mM NaN_3, 2% PVP, 0.05% Tween 20 in PBS) and duplicated 100 μL aliquots of each plant were loaded on the ELISA plate and incubated at 37 °C for 3 h, washed 3 times with PBS-T. Secondary antibody (rabbit anti ZYMV CP conjugated with alkaline phosphatase) was added, diluted 1:2500 in conjugation buffer (3 mM NaN_3, 2% PVP, 0.05% Tween 20, 0.02% ovalbumin in PBSx10 and incubated 2 h at RT, following by 6 washes in PBS-T. Plate was dried and incubated with 0.7 mg/mL p-nitrophenyl solution made by dissolving p-nitrophenyl SigmaFast tablets (Sigma, Darmstadt, Germany) in Substrate Buffer (3 mM NaN_3, 10% diethanolamine). Color development was monitored using an ELISA Reader (Anthos Reader 2001, Biochrom, Cambridge, UK) at 405 nm. Known amounts of purified ZYMV were used to generate a calibration curve.

2.3. BAC Library Screening and Chromosome Walking

For chromosome walking, two BAC libraries were used. The first, from melon breeding line MR-1, was obtained from Clemson University Genomic Institute (CUGI), and contained 67,968 clones with an average insert size of 118 kb, representing $15\times$ coverage of the melon genome [39]. The second was developed at INRA-URGV, France, from the American Cantaloupe breeding line WMR 29 ([40]), and consisted of 32,632 clones (average insert size 100 kb, $7\times$ genome coverage).

The MR-1 BAC library, arrayed as DNA spots on Nylon filters, was initially screened with the *Zym*-linked CM-AG36 marker [34], amplified using primers Con-2R 5′CTTCCC GACCTATCAGTAC3′ and Con-8F 5′CCTTTGA-ACATAGGAATGAGGCA3′). In subsequent stages of chromosome walking, probes were made by PCR amplification of fragments from the sequenced BAC-ends. Probes were labeled with [α-^{32}P]dCTP using Klenow fragment and random hexamer primers (Roche, Basel, Switzerland) and hybridized with colony filters as described by [41]. Hybridized filters were washed and exposed for 1–4 days to an X-ray film (Kodak, Rochester, NY, USA). Clones giving visible hybridization signals were ordered from CUGI and used for additional walking rounds.

The WMR 29 BAC library was organized in 86 384-well plates, and a pooled DNA sample from each plate (384 individual clones) was prepared. PCR screening of 32,632 BAC clones was performed on the 86 DNA pools using specific primer-pairs. The individual clones of each positive pool were plated in a 24 column $\times$ 16 row pattern on large LB plates, and 24 PCR reactions on the pooled columns were performed. Colonies represented in the PCR-positive pools were individually amplified, in order to isolate a single positive BAC clone.

2.4. BAC End-Sequencing and Marker Development

For BAC-end sequencing, 100 mL of LB broth supplemented with 34 mg/L chloramphenicol (Sigma, Darmstadt, Germany) were inoculated with a single BAC colony and grown at 37 °C with 250 rpm agitation overnight. DNA was isolated using the Nucleobond AX 100 kit (Macherey-Nagel, Düren, Germany). The two BAC-end sequences were determined using Sp6 and T7 vector primers flanking the insertion site, using an ABI automatic sequencer (Applied Biosystems, Waltham, MA, USA). Based on the resulting sequences, PCR primers were designed, and the amplified fragments served as probes for subsequent BAC screening steps. The same primers were used to amplify the respective amplicon from the different mapping parents of populations 1–5 to search for polymporphism between pairs of parents, and develop cleaved amplified polymorphic sequences (CAPS) and derived cleaved amplified polymorphic sequence (dCAPS; [42]) markers for fine genetic

mapping of the locus on the different populations. This resulted in anchoring the BAC contig (physical map) to the genetic map that contained the *Zym* locus itself, culminating in determining a BAC clone that encompassed *Zym* between its two ends. Primers were designed using Primer3 (http://frodo.wi.mit.edu/primer3) to obtain a product size of approximately 300–500 bp. Table 2 shows the genetic markers developed in this study.

Table 2. Markers used in this study for genetic mapping of the *Zym* locus. Primer sequence, annealing temperature, amplicon size, and diagnostic restriction enzymes are given.

Marker Name	Primer Name	Primer Sequence 5′-3′	Tm (°C)	Size (bp)	Diagnostic Enzyme
183C5-T7	183C5F-T7	CCAAAAACACAAAGGAAGTTTATA	56	385	*Csp*6I
	183C5R-T7	AGAATCACTTGTAAACATAGCCTT			
90D15-sp6	90D15-FSP6	ACAAACGGATAAATGAAAAGGA	56–60	320	*Hind*III
	90D15-RSP6	ACTTCCTGCTAGTGGCGTTT			
M2-new	M2Fnew	GAATCATTTAACAAAACAAAAGTA	55–60	1306	*Taq*I, *Mse*I, *Tai*I
	M2-R	GCATCTCTTATTAGTTTTCGAG			
Z1	Z1-F	GTATCGAGTTTCTCCCTGATCCT	53	1112	*Tru*I
	Z1-R	TGTGTGTTGGACTTGTGATTTGT			
Z3	Z3-F	ACAATCATTTTCTACAACGGAACA	60	1160	*EcoR*V, *Tas*I
	Z3-R	GGATCAGGGAGAAACTCGATACTA			
60A10-sp6	60A10-F-SP6	TTCCAACGATTTTTCATCACC	52	412	*Taq*I
	60A10-R-SP6	TGCAAATCCTTTGGCAAATA			
60A10-F4-sp6	60A10-F4-SP6	TTCGAAAGTTGGAATTACATTGG	55–57	385	*Bfm*I, *Hinc*II, *Apo*I, *Hinc*II
	60A10-R4-SP6	GGTGATGAAAAATCGTTGGAA			
MA	MA-F	CACTTGGCAGT CCCATTAGTCTTTGAC	60	1395	*Msp*I, *Xpa*I
	MA-R	GAAGGAGAAGTAATTGGTCGAGATGAT			
MB	MB-F	GTGAAG ATGATACTCG TGTATAACC	60	1404	*Taq*I, *Tas*I
	MB-R	GAACACGATATTATGGTTAAATCC			
70P22-T7	70P22-F-T7	TTTCTGTTGTTTTCTTTTCCTTGC	56	345	*Sal*I
	70P22-R-T7	CCATTGTATTGTTGTTGGTGGAGA			
M3	M3-F	CTTCATGAGG GTGGACAGAG GAAAG	55–56	1161	*Sat*I
	M3-R	CTATGTTCTTTCATGATCGCTC			
Z2	Z2-F	TTAAATTTGGGTTTTCCATTGACT	55	1054	*Fsp*BI, *Tru*I, *Tai*I
	Z2-R	ATTAAGGGTTTGAATTGCAAATGT			
M4	M4-F	GATTTACAAAATTAGTTGAC AAG	60	1653	*Alu*I
	M4-R	GTTAAAATTAGGTTTCCACAAC			
M6	M6-F	CTAACGTT TAGTTTGAAC AACC	55–56	1378	*Tai*I
	M6-R	GAGGCATTGGCATCCAAAAACTC			
90D15-T7	90D15-FT7	GCCTAGCAGTGGATTTTTCG	59	471	*Tas*I
	90D15-RT7	TCGAAACTTTTAAAGGCAGCA			
92C12-T7	92C12-FT7	ACTTTCCATCCCACCAATGCT	56–60	200	PCR product presence
	92C12-RT7	AATCCCCACTTTCTTGGTGGA			
35H2FN-T7	35H2FN-T7	TTCTTTGTCTCCTTTCTCCTC	56	415	*Dra*I
	35H2R-T7	ATATTGGTTTGGTCGGTTGG			
35H2F4-T7	35H2F4-T7	TGAATCGAGAGGGGTCATTG	56	330	*Hph*I
	35H2Rx-T7	ATATCTGAGGTACGAAGGAGAAAC			

2.5. BAC Contig Assembly Using Clone Fingerprinting and PCR Analysis

For fingerprinting and PCR analysis of BAC clones, we prepared DNA from small, 3 mL bacterial cultures, using standard alkaline lysis plasmid miniprep method. BAC DNA (1 µg) was digested with *Eco*RI or *Hind*III restriction enzymes, and the fragments separated by electrophoresis on 1% agarose gels. BAC clones were ordered with respect to each other to form a contig by visually comparing the overlaps between their fingerprint patterns, and by performing reciprocal PCR reactions to amplify BAC-end fragments from the different BAC DNA preps, and assess whether the end-sequences of each clone are present in the other members of the contig.

2.6. Whole BAC Sequencing and Sequence Assembly

BAC plasmid DNA was extracted from the two selected BAC clones that contained the *Zym* locus using BACMAX^TM DNA Purification Kit (Epicentre Biotechnologies, Madison,

WI, USA). Plasmid DNA (4 μg from each clone) was sent to the DNA Services Laboratory, Center for Comparative and Functional Genomics, University of Illinois. Sequencing with Roche 454 Titanium Sequencing System was performed after tagging each fragmented clone with a specific adaptor, mixing and running them together on a single lane; the two "sequence libraries" were later sorted according to their tags. Vector sequences, bacterial sequence contamination, and low-quality sequences were removed using the SeqClean software (http://compbio.dfci.harvard.edu/tgi/software/), run using a minimum read length parameter of 30. The raw sequences were screened against the NCBI UniVec Database (Build 6.0), as well as the specific vector sequences of the two BAC clones, namely pIndigoBAC536 for clone 90D15 (melon genotype MR-1), and pBeloBAC11 for clone 34-18-1 (genotype WMR 29). The resulting filtered Fasta file and its corresponding quality file were used as input to the assembly process, carried out by the GS Assembler Version 2.5.3 (Roche, Basel, Switzerland), using the following default parameters: seed step 12, seed length 16, seed count 1, minimum overlap length 40, minimum overlap identity 90%, alignment identity score 2, and alignment difference score −3. This resulted in a few sequence-contigs per clone, and the remaining gaps between contig ends were closed by PCR amplification using opposing primers from the two neighbor contigs and Sanger sequencing of the PCR fragments.

2.7. Sequence Annotation and Comparison

Predicted genes were located on the assembled BAC clone 34-18-1 sequence. For this purpose, we applied BLAST analysis of the BAC sequence against the nr nucleotide collection of NCBI, then against the melon ESTs collection, and finally against the cucumber genome at the Cucurbits Genomics Database (http://www.icugi.org/) and noted regions of homology to expressed genes. The translated BAC sequence was then assessed manually using BLASTx against the nr protein database of NCBI, and exon boundaries were identified such as to maximize homology of the putative coding sequence to known proteins. Intron/exon junctions were determined by aligning available melon cDNA sequences with the BAC genomic sequence, and finely adjusted according to the consensus plant splice sites. Annotation was finally refined based on RNA seq data made available at the Cucurbit Genomics database (http://cucurbitgenomics.org/). Protein domains were identified in the translated protein sequence by the InterPro software (http://pfam.sanger.ac.uk/search) that searches for known protein domains in the HMMPfam database [43]. Potential coiled-coil domains were predicted with MARCOIL (http://toolkit.tuebingen.mpg.de/marcoil), an HMM-based (Hidden Markov Model-based) program. The two assembled BAC sequences were deposited in the GenBank database as accessions KY643743 (clone 34-18-1) and KY643744 (clone 90D15). To position the two BAC sequences on the published melon genomes we used MUMmer3.23 [44], http://mummer.sourceforge.net/. To locate protein genes within the syntenic regions in the different genomes and compare them to our BAC annotation, we used Exonerate 2.2.0 [45].

2.8. Amplification and Sequencing of Zym Alleles from a ZYMV Resistant Genotype

In order to discover the genetic polymorphism that could give rise to the different resistance/susceptibility phenotypes, we sequenced the 18 kb *Zym* genomic region defined by the closest genetic markers in the resistant melon genotype, PI 414723. Fourteen pairs of primers were designed, each amplifying ~1200 bp, with an overlap of ~200 bp between adjacent fragments. Single PCR fragments were produced, directly sequenced and manually assembled. The assembled sequence was deposited as GenBank accession KY643745, and aligned with the other two sequences of this region (from clones 34-18-1 and 90D15) using CLUSTALW (http://www.clustal.org/).

2.9. QTL Mapping of Zym with High Density Markers Derived from RNAseq

This experiment, aimed at saturating the *Zym* locus with additional SNP markers, was run as a parallel approach to the main chromosome walking and fine mapping experiment

described in the previous sections. It only involved Population 1 (Table 1), that was grown and phenotyped for ZYMV as described in [35]. RNA-Seq based QTL analysis was performed by NRGene LTD (Nes Ziona, Israel) using 79 families of Population 1 and ca. 58,000 SNPs, as described by [36].

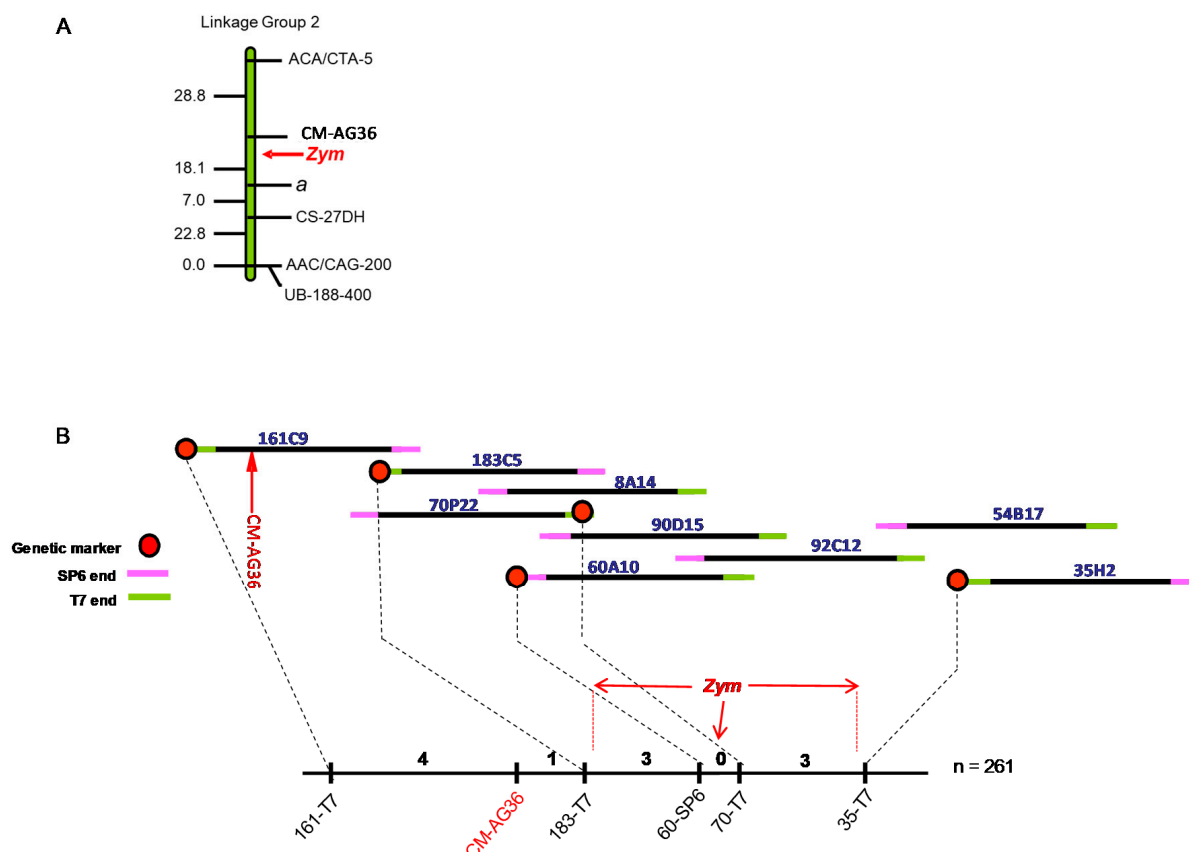## 3. Results

3.1. ZYMV Resistance in PI 414723

PI 414723, an Indian melon landrace belonging to the *Cucumis melo* var. *momordica* group, serves as a source of monogenic dominant resistance to ZYMV [30]. This resistant accession does not develop any mosaic symptoms. It may either remain symptomless, or react to ZYMV by developing necrosis of the leaves, stems, and stunting or even death of the plant. Such reaction is probably due to environmental conditions/genetic interactions that are poorly understood. We wished to determine whether the *Zym* gene provides tolerance while allowing viral spread, or completely restricts viral multiplication and systemic spread. We therefore used polyclonal antibodies against the ZYMV coat protein to monitor virus spread in resistant PI 414723 and susceptible Top Mark melon, and two homozygous resistant and homozygous susceptible recombinant inbred lines (RIL), respectively, derived from Population 2 (Table 1). Plants were inoculated in their cotyledons, and systemic leaves were sampled 6, 13, and 28 days post inoculation (dpi). Figure 1A–E shows examples of resistant and susceptible phenotypes, respectively. Resistant plants inoculated with ZYMV had very low to undetectable virus titers ($OD_{405} \leq 0.02$), similar to the values of non-inoculated control plants (Figure 1F). OD values of inoculated Top Mark plants and susceptible progeny reached 0.4–0.5, that corresponded approx. to 2.5–5 mg/mL of virus according to our coat-protein-based calibration curve, increasing sharply between 6 and 13 dpi, later remaining constant, or decreasing by 28 dpi. We concluded that *Zym*-encoded resistance effectively blocks viral spread in the plant.

3.2. Chromosome Walking towards the Zym Locus

The *Zym* locus that confers monogenic dominant resistance towards ZYMV has been previously mapped to Linkage Group II of the melon genetic map, and an SSR marker, CM-AG36, mapped in close proximity (~2 cM) to *Zym* [8,34,35]; Figure 2A). In the present study, we have undertaken physical mapping of the *Zym* gene in order to generate a high-resolution map, identify candidate genes, and eventually clone *Zym*. Chromosome walking was initiated using the CM-AG36 marker as a starting point. On the other side of *Zym*, the *andromonoecious gene (a)* was distantly linked (18 cM from CM-AG36, [46], but no closer marker was available to us (Figure 2A). A melon genomic BAC library from melon MR-1 was hybridized with the CM-AG36 DNA probe, and a first BAC clone 161C9 was identified (Figure 2B). This clone was verified by PCR amplification with specific CM-AG36 primers and by Southern blot hybridization with the CM-AG36 probe. The two BAC ends, "161C9-SP6" and "161C9-T7" were sequenced, and new probes were generated from the sequenced ends by PCR amplification, using sequence-specific primers. Clone-ends that did not overlap with previously isolated clones in the contig were positioned at the contig extremity, and were used to screen the library again; the clone order was also supported by BAC fingerprinting and Southern analysis. A total of nine walking steps resulted in a single contig of BACs (Figure 2B). In order to orient the contig with respect to the genetic map, we had to develop new contig-based markers and place them on the genetic map with respect to *Zym*. For this purpose, BAC-end sequences were amplified from all the parental genotypes of the different mapping populations. SNP discovered between the parental sequences served to develop new CAPS and dCAPS markers (Table 2). Initially, three melon recombinant inbred lines (RIL) populations where used, totaling 261 individuals (522 gametes; Populations 1–3, Table 1). All individual RILs were inoculated with ZYMV as reported [8,35]. They were screened with SSR marker CM-AG36 and five novel CAPS markers flanking the *Zym* locus (Figure 2B). Of these, markers 60SP6 and 70P22T7 co-segregated with *Zym* and could not be oriented with respect to the gene. At this stage

(Figure 2B), *Zym* was separated by 3 recombination events/261individuals from marker 183-T7 on one side, and 3 recombinations/261 individuals from marker 35H-T7 on the other side. However, to map the locus at high resolution, larger mapping populations were required. Table S1 shows the marker scores of informative progeny that served to construct the genetic map.


Figure 2. Mapping of *Zym* on melon linkage group 2. (**A**) Genetic map based on [34,46], that served as starting point for the chromosome walk described in this study. (**B**) First stage of choromosome walk resulting in a BAC contig and medium-resolution genetic map. The CM-AG36 marker sequence [34] was used as a first probe to screen a melon BAC library of the MR-1 genotype. For subsequent rounds of screening, probes were prepared by sequencing the SP6 and T7-oriented ends of the BAC inserts, and a contig of partially overlapping BAC inserts (horizontal lines) was generated. Several BAC-end sequences (marked by red circles) were used to generate polymorphic CAPS markers (Table 2) and these were used to screen mapping populations 1–3 (261 individuals, Table 1) and connect (dashed lines) the physical map (contig) to the genetic map, shown as a solid line, below; figures between markers represent the number of cross-over events. At this stage, *Zym* co-segregated with markers 60-SP6 and 70-T7, and was therefore delimited to the interval between markers 183-T7 and 35-T7.

3.3. Fine Mapping of Zym

For increased resolution, we extended our analysis to two additional populations (Table 1, Populations 4 and 5). Population 4 included 141 F2 plants from a cross between ZYMV-resistant PI 414723 and ZYMV-susceptible melon 'BIZ' [37]. The F2 plants were sampled for DNA and self-pollinated to obtain F3 families. Population 5 was a Backcross-1 (BC$_1$-S$_1$) population, composed of 1228 BC$_1$ plants from a cross between Védrantais (ZYMV susceptible) and PI 414723 (ZYMV resistant), backcrossed to PI 414723. BC1 plants were sampled for DNA extraction, and self-pollinated to obtain BC$_1$-S$_1$ families. This increased our combined mapping screen to a total of 1630 individuals. ZYMV resistance was only tested in individuals of populations 4 and 5 that exhibited a recombination event in the vicinity of the gene. To expedite identification of such individuals, we multiplexed markers 183C5-T7 and 35H2-T7, performing their amplification and restriction in a single-

tube reaction. We confirmed recombination by checking additional markers around the locus, and inoculated duplicate progeny samples of these individuals with ZYMV. In the F$_3$ families, progenies were either all-resistant, all-susceptible, or segregating at an approximate 3 resistant: 1 susceptible ratio, as expected. In the BC1-S1 samples, progeny samples were either all resistant, or segregating at an approximate 3 resistant: 1 susceptible ratio. We thus recovered two additional plants with a cross-over event between marker 183C5-T7 and *Zym*, and 18 with recombination between *Zym* and marker 35H2-T7 (Figure 3; Table S1).
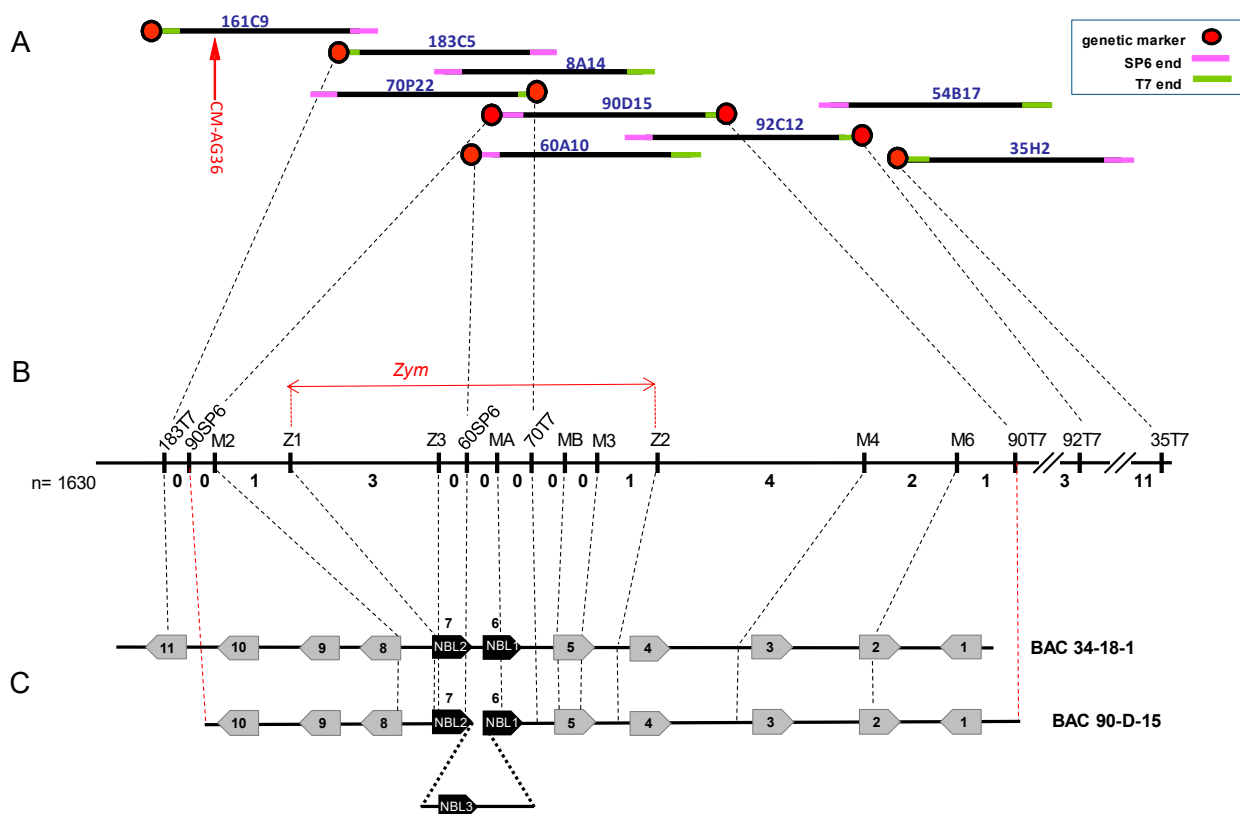
Figure 3. High-resolution physical and genetic map of the *Zym* locus based on five mapping populations and additional BAC-sequence markers. (**A**) Physical map made of BAC clones contig as in Figure 2B. Markers derived from BAC end sequences (Table 2) are shown as circles. (**B**) High resolution genetic map of the same interval. Map (solid line) is based on 1630 individuals from 5 mapping populations (Table 1), figures represent number of cross-over events. Dashed lines connect BAC end-markers with the genetic map. The two markers derived from BAC 90-D-15 map on both sides of *Zym*, at a distance of 11 and 4 cross over events, respectively, showing that *Zym* is encoded within this clone. Additional CAPS markers (M2, Z2 etc.) were derived from internal sequences of BAC clone 90-D-15, after its full sequencing. As a result, *Zym* co-segregated with markers Z3, 60-SP6, MA, 70-T7, MB, M3, and was delimited by markers Z1 and Z2. (**C**) Diagram of BAC clone 90-D-15 from melon MR-1, and the homologous clone 34-18-1 from melon WMR 29, with 11 hand-annotated ORF (drawn at approximate scale; direction with respect to BAC sequence is shown by arrow-heads, ORF details are given in Table 3). Dashed lines indicate CAPS markers location within BAC. Two NLR homologues in clone 34-18-1 and three in clone 90-D-15 are shown in black.

At this stage, we added three new CAPS markers derived from two BAC-ends, namely 90D15-SP6, 90D15-T7, and 92C12-T7 (Figure 3A, Table 2), to bridge the gap between markers 183C5-T7 and 35H2-T7. The individuals showing recombination events in this interval were screened. We found that markers 90D15-SP6 and 90D15-T7, derived from the two ends of a single BAC clone, mapped at a distance of four recombinants and eight recombinants, respectively, on both sides of Zym (Figure 3B; Table S1). We concluded that Zym was physically confined to a single clone. In an attempt to clone the locus from an additional melon genotype, we used the two BAC-end markers of clone 90D15

as probes, and screened a second BAC library, from melon genotype WMR 29, another ZYMV-susceptible breeding line. We isolated clone 34-18-1 that is shorter than 90D15, and contains only probe 90D15-SP6. We later found, by adding internal markers (see below), that Zym was contained also within clone 34-18-1 (Figure 3C).

Table 3. Gene annotation of BAC clone 34-18-11 (GenBank accession KY643743). Eleven gene coding sequences were hand annotated on the BAC sequence, their gene number on the published melon genome and their sequence homology revealed by BLAST search against the Swissprot database is indicated, as well as the position of the respective exons of the BAC sequence. Supplementary Table S2 provides their position on four published melon genomes.

№	Gene ID	Sequence Homology	Gene Model (Exon Positions on BAC Clone 34-18-1)
1	MELO 3C015360	TF IIIB 60 kD subunit	128..243, 1025..1105, 1335..1472, 1557..1580, 2041..2145, 2354..2407, 2961..3176
2	MELO 3C015359	His-containing phospho-trasferase	8369..8440, 8743..8815, 9706..9774, 9933..10,063, 10,571..10,633
3	MELO 3C015358	Autophagy 18H-like protein	18,420..18,424, 19,353..19,877, 19,977..20,104, 24,688..24,863, 24,942..25,736, 25,813..26,058, 26,831..27,265, 27,612..28,070, 29,451..29,654
4	MELO 3C015357	NAC domain Transcrtiption Factor	36,438..36,710, 36,919..37,188, 37,439..37,765, 37,859..37,984, 38,217..38,491, 38,571..38,748
5	MELO 3C015355	NAC domain Transcrtiption Factor	404,93..40,840, 40,960..42,132, 42,340..42,654, 42,742..42,882, 43,402..43,664, 43,738..43,915
6	MELO 3C015354	CC-NBS-LRR (NBL1)	45,722..49,075
7	MELO 3C015353	CC-NBS-LRR (NBL2)	52,452..55,706
8	MELO 3C015352	Dihidroorotate Dehydrogenase	58,807..58,941, 60,448..60,531, 61,677..62,000, 62,216..62,470, 63,432..63,512, 63,593..63,730, 63,940..64,077, 64,813..64,848, 64,967..65,068, 65,791..65,862
9	MELO 3C015351	Superoxide Dismutase	68,656..68,712, 69,076..69,183, 70,036..70,230, 71,369..71,536, 71,942..72,016, 72,091..72,117, 72,209..72,232, 72,771..72,893
10	MELO 3C015350	sugar transporter ERD-like	73,954..74,019, 75,011..75,073, 75,370..75,459, 75,558..75,626, 76,044..76,100, 76,193..76,258, 76,956..77,036, 77,122..77,181, 77,548..77,640, 77,736..77,825, 77,930..78,010, 78,098..78,133, 78,218..78,283, 78,366..78,419, 78,519..78,578, 78,901..78,960, 79,262..79,378, 79,468..79,593
11	MELO 3C015349	sugar transporter ERD-like	81,079..81,225, 81,969..82,031, 82,758..82,844, 82,993..83,055, 83,542..83,604, 83,711..83,773, 84,162..84,248, 84,336..84,392, 84,701..84,793, 84,876..84,959, 85,289..85,381, 85,856..85,942, 86,026..86,085

3.4. Clones 34-18-1 and 90D15 Contain a Small Cluster of Resistance Gene Homologs

The two clones, 90D15 from melon MR-1 and 34-18-1 from melon WMR 29, were fragmented, individually tagged, and subjected to 454 sequencing. This resulted in 65,120 reads for clone 90D15 and 26,301 reads for clone 34-18-1, of 490 bp average length and an average guanine+cytosine (GC) content of 38%. Sequences were assembled into a single contig representing each clone and hand-annotated as described in the Methods. The two BAC sequences were deposited as GenBank accessions KY643743 (clone 34-18-1) and KY643744 (clone 90D15).

The contiguous sequence of clone 34-18-1 (from melon WMR 29) is 86,629 bp long and contains eleven open reading frames (ORF) with homology to known proteins in the GenBank database (Table 3; Figure 3C). Among them, two ORF, 5 and 6, share homology with typical resistance genes of the coiled coil- nucleotide binding site—leucine rich repeat family (CC-NB-LRR, abbreviated as NBL). These genes were designated *NBL-1* (MELO3C015354 in the published melon genome) and *NBL-2* (MELO3C015353). Adjacent to the NBL pair, ORF 4 and 5 encode two transcription factors from the NAC family (MELO3C015355, MELO3C015357). More upstream we find proteins with similarity to autophagy-related protein 18H, a phospho-transferase and a Type IIIB transcription factor. Downstream of the NBL proteins we see ORF encoding dihidroorotate dehydrogenase, superoxide dismutase and two sugar transporters. Clone 90D15, from melon MR-1, is

longer (105,287 bp), and most of its sequence overlaps with clone 34-18-1 (Figure 3C); its annotation revealed a similar gene content in the shared region, except for a unique insertion of ca. 6000 bp within the NBLs cluster, harboring a third NBL gene, *NBL-3*. The NBL-encoding genes are arranged in a head-to-tail orientation, separated by ca. 3 kb between them. They share a similar gene model, according to our annotation, consisting of a single predicted exon with no introns. RNAseq data available at the melon genome site (http://cucurbitgenomics.org/JBrowse) suggests that the two genes are expressed, but transcripts of *NBL-1* are less abundant then those of *NBL-2*. We then positioned our two BAC sequences, and the hand-annotated ORF, on chromosome 2 of the four different published melon genomes, to facilitate their localization on each genome. The full coordinates are shown in Table S2. We noted full conservation of gene content and orientation (except of a sugar transporter gene not found in DHL92), between BAC 34-1-18 from melon WMR-29 (a *cantalupensis* reticulated genotype) and the genomes of melon DHL92 [3], Japanese reticulated melon Harukei-3 [4], and Chinese sweet melon Paizawat [6], respectively. Interestingly, in the genome of melon HS, a *Cucumis melo var conomon* accession [7], the region was fully colinear with BAC clone 90D15 of melon MR-1, and contained the third *R*-gene homologue, *NBL-3,* as an insertion between *NBL-1* and *NBL-2*, similar in size and orientation to the one found in MR-1, while all other genomes only had *NBL-1* and *NBL-2*. Thus, the two *Zym*-locus variants that we describe in this study have been confirmed in four additional genotypes. We carefully examined the intervals between the candidate genes and their surrounding sequences and found no additional NBL family members or rearrangements in the four published genomes.

3.5. Candidate Genes for the Zym Locus Determined by the Closest Flanking Markers

At this stage, Zym was delimited by the two markers prepared from the ends of BAC 90D15-SP6, and such interval contained 10 ORF (Figure 3C). To further increase the resolution of our physical map and pinpoint fewer gene candidates, we developed additional polymorphic markers based on internal BAC sequence: these were designated M2, M3, M4, M6, Z1, Z2, and Z3 (Table 2), and were mapped on recombinant individuals from all five populations (Table S1). Among these, 12 individuals displayed recombination events between markers 90D15-SP6 and 90D15-T7, enabling the dissection of the annotated BAC sequence by internal recombination events. The two flanking CAPS markers that show recombination events with Zym are Z1 (3 recombinants/1630 plants) and Z2 (1/1630), showing that Zym is delimited by these two markers. This region is ca. 17,600 bp-long in clone 34-18-1 and contains the *NBL-1* and *NBL-2* candidates, as well as the adjacent NAC transcription factor-2 (Figure 3); all three represent therefore viable candidates for Zym. The other markers that were developed for the interval between markers Z1 and Z2 co-segregated with Zym, precluding further identification of a single candidate gene.

3.6. QTL Approach with Saturated SNP Detection Supports Genetic Mapping

As a complementary approach for candidate gene identification, we saturated the *Zym* locus with SNP markers obtained by high-throughput mRNA sequencing, coupled with powerful computational analysis [36]. The analysis was part of a parallel study that involved only Population 1 (Table 1), that had been phenotyped for ZYMV resistance [35]. Samples of mature fruit of the parental lines, F1 and 79 of the RIL were analyzed by RNA-Seq. Over 58,000 SNPs derived from the RNA-Seq were used for QTL analysis. We defined a major QTL for ZYMV resistance (LOD 10.18, $r^2 = 0.41$), representing *Zym*, in the expected region of chromosome 2 (Figure 4), with a QTL interval of 19 annotated genes and a bin of 12 genes at the peak (genomic location 921342–988427; *MELO3C015342-MELO3C015353*). The QTL includes *NBL-1*, *NBL-2* and *NAC-TF-2*, with the estimated peak encompassing *NBL-1*, strengthening our findings; however, despite the large amount of markers, the paucity of cross-over events in the single population prevented better definition of a gene candidate.
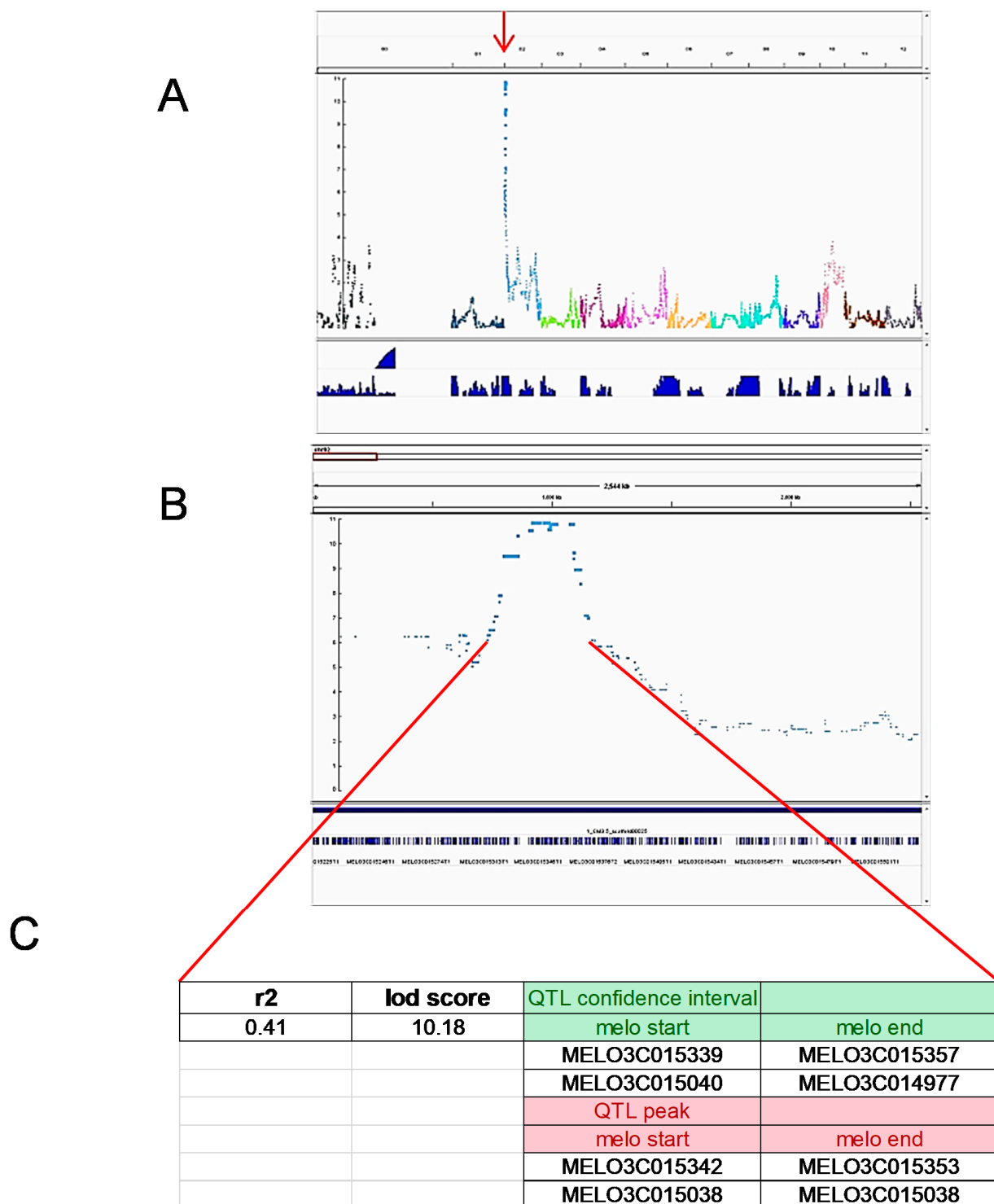
Figure 4. Mapping *Zym* as a QTL using saturated SNP discovered by high-throughput RNA sequencing. Analysis was performed by NRGene LTD (Nes Ziona, Israel) using 79 families from Population 1 and ca. 58,000 SNPs, as described by [36]. (**A**) View of 12 melon chromosomes (*X*-axis) depicted by IGV (Integrative Genomic Viewer, [47]), showing *Zym* QTL peaking on chromosome 2 (*Y*-axis is the LOD score of QTL). (**B**) Zoom-in view on the *Zym* peak. (**C**) QTL delimitation and confidence scores, delimited by the genes annotated at the borders and around the QTL peak.

3.7. Sequencing the Zym Locus from a ZYMV-Resistant Genotype

Comparison of susceptible and resistant alleles of an *R* gene could yield insight on the molecular basis of resistance. We therefore amplified by PCR partially overlapping

fragments from ZYMV resistant melon PI 414723 that cover the whole region between markers Z1 and Z2, that genetically delimits the *Zym* locus. We sequenced the fragments and assembled them into a contiguous 18,420 bp-sequence. Annotation of the sequence indicated that it contains the same pair of *NBL* genes and a *NAC* homologue as in clone 34-18-1, and has no additional NBL family members. The sequence was deposited as GenBank accession KY643745.

3.8. Protein Motifs and Polymorphism of Zym Candidates NBL-1, NBL-2 and NBL-3

While we could not exclude the NAC domain transcription factor as a *Zym* candidate based on genetic mapping, we examined in detail the sequences of the likely candidates, *NBL-1*, *NBL-2*, and (in melon MR-1) *NBL-3*, that form a small cluster of resistance gene homologues.

Their encoded protein sequences, consisting of ca. 1100 amino acids, contain typical CC, NBS, and LRR domains with known motifs, organized as a single exon. Figure S1 depicts the nucleotide and amino acid alignment of *NBL-1* and *NBL-2* in three genotypes, highlighting the conserved protein domains that we identified using bioinformatics tools such as Pfam and InterProScan (see Methods). Conserved motifs characteristic of the NBS domain, with its two subdomains, ARC1 and ARC2, including the P-loop, kinase-2, RNBS-B, GLPL, and MHD motifs [48], were identified. In the LRR region, we found two leucine rich repeats in *NBL-1* and three in *NBL-2*, 22–24 aa long.

Homology between the NBL paralogues is high: *NBL-1* and *NBL-2* display 88% nucleotide identity in their coding region, and 80% amino-acid identity (Table 4). The additional paralogue, *NBL-3*, found only in melon MR-1, is closer to *NBL-2* (86% amino acid identity), compared to *NBL-1* (81%). Similar values were also calculated between the *NBL-1* and *NBL-2* sequences in the other genotypes, MR-1 and PI 414723, that do not possess *NBL-3*. Interestingly, the amino acid sequences are less conserved than the nucleotide sequences, consistent with an evolutionary drive for protein diversification.

Table 4. Sequence homology between three NBL paralogues in the *Zym* locus of melon MR-1 (clone 90D15). Percent identity of nucleotide coding region is shown, with percent amino-acid sequence identity given in parentheses.

	NBL Paralogue Identity, %	
Gene	*NBL-2*	*NBL-3*
NBL-1	88 (80)	88 (81)
NBL-2		92 (86)

We examined the DNA and amino acid sequence diversity of *NBL-1* and *NBL-2* among the three melon genotypes. In Figure S1, the polymorphic residues are shaded and the coloring highlights which genotype has a diverged residue compared to the other two. Table 5 summarizes these data. Both genes had high rates of polymorphism, with *NBL-2* being twice more diverged (126 polymorphic amino acids, compared to 63 in *NBL-1*). The ratio between DNA polymorphism that causes amino acid substitutions (non-synonymous) to silent DNA polymorphism (Ka/Ks) is 1.1 in *NBL-1* and 2.8 in *NBL-2*. Figure 5 is a schematic representation of the amino acid polymorphism along the two proteins, and shows another striking difference between the two genes. In *NBL-1*, 53 of the 63 substitutions are found in the amino-terminal half of the protein encompassing the CC and NBS domains, and only 10 in the LRR containing portion, while in *NBL-2* most polymorphism (115 of 126 residues) is found in the LRR-containing portion and only 11 in the amino-terminal half.

We asked whether we could find amino acid substitutions that differentiate *NBL-1* and *NBL-2* alleles of the two ZYMV susceptible genotypes, MR-1 and WMR 29, from those of the ZYMV resistant genotype, PI 414723. In *NBL-1*, 57 amino acid substitutions were unique to PI 414723, and only 2 and 4 were unique to WMR 29 and MR-1, respectively

(Table 5, Figure S1). In *NBL-2* there were numerous unique substitutions in each of the three genotypes, with PI 414723 still being the most diverged (43, 39, and 60 genotype-unique residues in WMR 29, MR-1, and PI 414723, respectively). These data point at interesting patterns of evolution acting on the two genes. However, because of the many polymorphic sites differentiating PI 414723 from the two susceptible genotypes in each gene, no single substitution could be designated as a "candidate causative polymorphism" that could explain the resistant phenotype.

Table 5. Sequence diversity in the coding region of *NBL-1* and *NBL-2*, revealed among three genotypes, WMR 29, MR-1, and PI 414723. Protein and DNA sequences from MR-1, WMR 29, and PI 414723 were aligned (Figure S1 shows the full alignments), and polymorphic sites that differentiate at least one genotype from the others were noted. Small insertion/deletions were counted as a single polymorphism. Number of sites that differentiate a specific genotype from the other two are indicated.

| Sequence		Total Length	Polymorphic Sites No.	Unique to WMR 29	Unique to MR-1	Unique to PI 414723
NBL-1	DNA	3354	120	4	5	111
	Protein	1118	63	2	4	57
NBL-2	DNA	3294	171	94	57	73
	Protein	1098	126	43	39	60
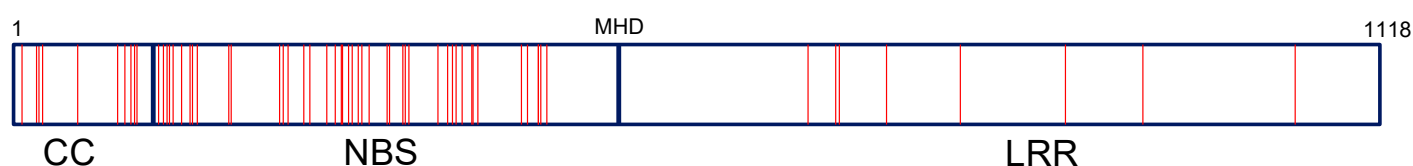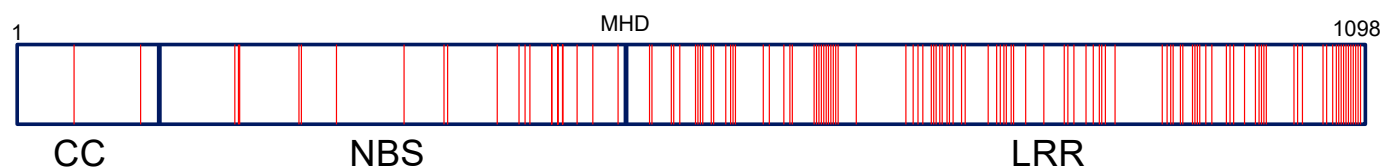
Figure 5. Distribution of polymorphic acids in the *NBL-1* and *NBL-2* predicted protein sequences among three genotypes. Protein and DNA sequences of MR-1, WMR 29, and PI 414723 were aligned (Figure S1) and non-synonymous polymorphic sites that differentiate at least one genotype from the others are shown as red bars on the boxes representing the two proteins. The sequences were divided into three regions that encompass the coiled coil (CC), nucleotide binding site (NBS), and leucine rich repeat-containing (LRR) regions, respectively; MHD motif is shown as well. Small insertion/deletions were counted as a single SNP.

3.9. Synteny of the ZYMV Locus with a Homologous Genomic Region in Cucumber

We wished to assess the extent of synteny between the melon *Zym* genomic region and the homologous region in the closely related species, cucumber (*Cucumis sativus*). We searched the published Chinese Long cucumber genome [49] with the *Zym* encompassing BAC sequences from melon, and identified in cucumber chromosome 1 a region with high synteny to the melon *Zym* region. Most of the annotated genes are present in the two species in the same order (Figure 6). Interestingly, cucumber has a single CC-NBL homolog in a reverse orientation, inserted between the two NAC genes, suggesting a duplication and inversion in the melon lineage.
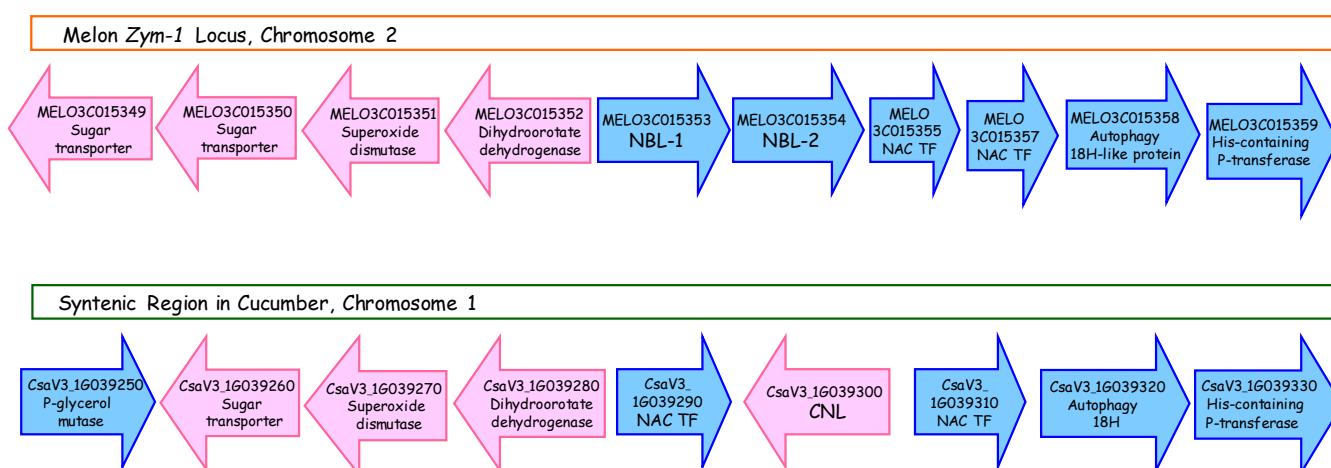
Figure 6. Synteny of the *Zym* genomic region between melon and cucumber. Schematic representation of the *Zym* region of WMR 29 melon on chromosome 2, with the syntenic region in cucumber. The cucumber sequence was unloaded from the published Chinese Long cucumber genome ([49], http://cucurbitgenomics.org). The genes annotated in each region are depicted schematically as arrowheads, with color representing gene orientation, to show similarity in gene content and overall genomic organization.

4. Discussion

Breeding disease resistant cultivars is a long range effort that can be facilitated by development of tightly linked markers to accelerate progeny selection during breeding cycles. Such markers also serve as physical starting points towards the molecular isolation of the resistance genes. Cloned *R*-genes provide biological and evolutionary insight to the arms race between host and pathogen and can be used in biotechnology to engineer resistance [50].

Despite the economic importance of *Cucumis melo*, only a handful of *R*-genes have been cloned in this species. These included *Vat*, conferring resistance to aphids [51], *Fom-2*, conferring resistance to *Fusarium oxysporum* f. sp. *melonis* races 0 and 1, [52], and the head to head oriented pair of R-genes, *Fom-1* and *Prv*, that confer resistance to Fusarium races 0 and 2, and to the potyvirus *Papaya ring spot virus*, respectively (Brotman et al., 2013). These four genes encode typical R-gene homologues of the NBS-LRR super family. In addition, recessive resistance genes have been identified, namely *nsv*, controlling resistance towards the Melon necrotic spot virus, that encodes a translation elongation factor [53], downy mildew resistance genes encoding photorespiratory amino transferases [54], and *cmv1*, that encodes a vacuolar sorting protein [17]. Our study reports map-based cloning of a locus that confers resistance towards an important potyvirus, ZYMV, that causes severe economic losses to all cultivated cucurbits [20]. Transgenic cucurbits were obtained that express viral proteins or RNA molecules rendering them ZYMV resistant [31–33]. Nevertheless, understanding and utilizing natural variation in this trait is of great interest.

Melon PI 414723, an Indian accession of the *C. melo* var. *momordica* botanical group [29], is the best characterized ZYMV resistance source in melon, and the gene has been designated *Zym* [30]. In an early study, two additional genes segregated in specific crosses and contributed to resistance [55]. However, in all subsequent studies, resistance was mapped as a monogenic, dominant trait [8,34]. Such discrepancy could have been caused by the different susceptible parents used for mapping, or the specific breeding line derived in each study from the presumably heterogeneous PI 414723. Resistance derived from PI 414723 is accompanied by local necrosis of the stems and leaves, often leading to growth arrest, whereas susceptible plants display prominent mosaic symptoms and severe distortion of leaves and fruit. The extent of necrosis apparently depends on the temperature and genetic interactions, being less severe and even absent in certain F_3 or RIL families, or under certain poorly-defined environmental conditions (our unpublished observations). Another potyvirus resistance gene of melon, *Prv*, has two different resistance alleles. *Prv*[1]

confers symptom-less immunity, whereas *Prv*^{2}, coming from the same PI 414723, shows a necrotic type of resistance [30]. To elucidate the type of ZYMV resistance from PI 414723 we used ELISA and showed that ZYMV spread to systemic leaves is reduced to undetectable levels (Figure 1). On the other hand, we did observe in some cases that systemic leaves from resistant plants with undetectable titer could still infect susceptible test-plants ([56]). The necrotic nature of this resistance source renders it less attractive to breeders. Screens for additional sources have been conducted [57] and new potential sources were reported [58], but at present, it is important to understand PI 414723 necrotic reaction and develop ways to control it, or select genetic backgrounds that minimize such effect. Recently, deregulation of *R*-gene action leading to autoimmunity, manifested as necrosis and dwarfism, has been the object of numerous studies [59]. It is now increasingly evident that *R*-gene action is affected by temperature [60], and it will be useful to elucidate environmental effects on *Zym* action.

Using ~1600 segregating progeny from five different mapping populations, and performing a chromosome walk using two BAC libraries, the locus has been narrowed-down to a physical interval of 17.6 kbp on linkage group 2, between markers Z1 and Z2 (Table 2, Figure 3). In the process, numerous useful CAPS markers have been generated and tested, which could assist ZYMV resistance breeding in different genetic backgrounds and breeding platforms. The two BAC clones have been completely sequenced and hand-annotated. The smallest *Zym* interval contains three open reading frames in melon WMR 29, two of which encode tandem-arranged homologues of the coiled-coil-NBS-LRR subfamily, designated *NBL-1* and *NBL-2*. In melon MR-1 there is a third homologue, *NBL-3*. The interval also contains *NAC-2*, encoding a NAC domain transcription factor. NAC domain proteins belong to a large family of plant-specific transcription factors (ca. 150 members in rice), involved in plant development, senescence, and defense [61,62]. A well-studied member is Arabidopsis ATAF2 that interacts with TMV replicase, and its targeting by the virus was proposed to attenuate plant defense [63]. Other interactions of NAC TF with viral proteins that infect tomato and wheat, respectively, have been described [64,65]. It cannot be excluded at this point that the *Zym*-locus NAC could play a role in ZYMV resistance, although the two NLR homologs stand out as more likely candidates. Saturation of the locus with SNP markers in a single population of 79 plants pointed at the same region and supported our mapping (Figure 4), but provided no additional resolution, because the cross over events found in this population are not very close to *Zym*.

We sequenced the same interval also in ZYMV resistant melon PI 414723, and found that it contains *NBL-1*, *NBL-2*, and *NAC-2*, but not *NBL-3*. We also examined the interval in four recently published melon genomes and found no additional ORF or rearrangements of the locus. Comparing the DNA and predicted protein sequences of the *R*-gene homologues *NBL-1* and *NBL-2* across genotypes revealed extensive DNA and amino acid polymorphism between them; therefore, we could not pin-point specific sequence variation that could account for resistance of PI 414723, such as a dysfunctional substitution in the susceptible genotypes. Nevertheless, the patterns of variation across the two genes and three genotypes (Figure S1 and Figure 5) are interesting and suggest that these genes are under strong selection. The two genes are very similar (88% nucleotide identity, 80% amino acids identity) and must have resulted from a recent duplication, but each one has been differentially shaped by selective forces. In *NBL-1*, most of the amino acids polymorphism is found in the N-terminal half of the protein, including the CC and NBS-ARC domains, and very few substitutions differentiate the LRR regions of the three genotypes. While the LRR domains of NLR proteins are considered to mediate recognition and expected to undergo diversifying selection during plant–pathogen arms race [66], it is clear that the other domains must coevolve and diverge as well, to develop and maintain important interactions, with proteins such as helper NLR, guardee proteins, and pathogen Avr factors [67]. The large majority of polymorphic sites (111 of 120) distinguish PI 414723, the resistant genotype, from the two susceptible genotypes, MR-1 and WMR 29. The numbers of synonymous and non-synonymous DNA substitutions in the coding sequence

are near equal, suggesting moderate diversifying selection over the entire *NBL-1* protein (Ka/Ks = 1.1). *NBL-2*, on the other hand, has a Ka/Ks ratio of 2.8, suggesting stronger selection for diversification. The distribution of protein substitutions along the protein is opposite to that of *NBL-1*, with most diversity found in the LRR-half of the sequence, and numerous substitutions distinguishing each of the three genotypes (Table 5, Figure 5). In addition, *NBL-2* has been duplicated in MR-1, giving rise to *NBL-3*, which is very similar to *NBL-2* (92% nucleotide identity). The diversifying forces acting on this region are also apparent from the alignment of the melon *Zym* locus with the syntenic region in cucumber, found on chromosome 1. While the gene content and orientation are strictly conserved in this region between the two species (Figure 6), the small *R*-gene cluster within the conserved region is more dynamic, with only one NLR in cucumber compared to two or three in melon, the gene being inversely oriented and translocated with respect to the adjacent *NAC-TF* genes.

ZYMV attacks different *Cucurbitaceae* species, but it appears that melon and cucumber have evolved separate ZYMV resistance genes. The functional specificity of cucumber CsaV3_1G039290, the NLR homologue of melon *NBL-1* and *NBL-2* (Figure 6), is presently unknown, as is the function of the vast majority of NLR proteins in any plant species. A recessive ZYMV resistance gene, *zym*, has been described in cucumber [68], that confers resistance also to other potyviruses. It mapped to cucumber chromosome 6 at high resolution and found to encode a vacuole sorting protein, VPS4-like [69]. Such proteins were shown to interact with endosomal complexes required for virus multiplication. Interestingly, a melon homologue of VPS-4 was recently mapped and identified as a recessive resistance gene against another virus, CMV [17,70].

In conclusion, in this study, we cloned the *Zym* locus of melon by high-resolution mapping and narrowed the locus to a ~18 kb interval that contains two NLR homologs and a NAC transcription factor. To validate *Zym* experimentally, one should use CRISPR-Cas9 or other methods to mutagenize the candidates in a resistant genotype background and see whether resistance has been abolished. Despite many efforts, melon is still considered a recalcitrant species for genetic transformation ([71,72]. Fortunately, the *Zym* allele has been bred in a Charéntais type genetic background, which is relatively amenable to Agrobacterium mediated transformation. In addition, we could over-express melon *NBL-1* and/or *NBL-2* from PI 414723 in cucumber, which is easier to transform, and generate dominant resistance to ZYMV in this species.

Author Contributions: Conceptualization, R.P.-T., N.A.-B. and Y.G.; methodology, A.G.-O., A.B., C.T., N.K., R.H.-B., T.D. and C.D.; investigation, R.P.-T., Y.G., I.K., N.A.-B., Y.B. and R.H.-B.; resources, M.P., C.D., C.T., A.B., A.G.-O. and Y.B.; data curation, T.D., N.A.-B., R.P.-T. and I.K.; writing—original draft preparation, R.P.-T. and N.A.-B.; writing—review and editing, R.P.-T.; supervision, R.P.-T. and N.K.; project administration, R.P.-T. and I.K. All authors have read and agreed to the published version of the manuscript.

Data Availability Statement: The BAC sequences reported in this study are available as BenBank accessions KY643743, KY643744 and KY643745.

Conflicts of Interest: The authors declare no conflict of interest.

References

1. Arumuganathan, K.; Earle, E.D. Nuclear DNA content of some important plant species. *Plant Mol. Biol. Rep.* **1991**, *9*, 208–218. [CrossRef]
2. Garcia-Mas, J.; Benjak, A.; Sanseverino, W.; Bourgeois, M.; Mir, G.; Gonźalez, V.M.; Heńaff, E.; Camara, F.; Cozzuto, L.; Lowy, E.; et al. The genome of melon (*Cucumis melo* L.). *Proc. Natl. Acad. Sci. USA* **2012**, *109*, 11872–11877. [CrossRef]
3. Castanera, R.; Ruggieri, V.; Pujol, M.; Garcia-Mas, J.; Casacuberta, J.M. An improved melon reference genome with single-molecule sequencing uncovers a recent burst of transposable elements with potential impact on genes. *Front. Plant Sci.* **2020**, *10*, 1815. [CrossRef] [PubMed]
4. Yano, R.; Ariizumi, T.; Nonaka, S.; Kawazu, Y.; Zhong, S.; Mueller, L.; Giovannoni, J.J.; Rose, J.K.C.; Ezura, H. Comparative genomics of muskmelon reveals a potential role for retrotransposons in the modification of gene expression. *Commun. Biol.* **2020**, *3*, 432. [CrossRef] [PubMed]
5. Yano, R.; Nonaka, S.; Ezura, H. Melonet-DB, a Grand RNA-Seq gene expression atlas in melon (*Cucumis melo* L.). *Plant Cell Physiol.* **2017**, *59*, E4. [CrossRef]
6. Zhang, H.; Li, X.; Yu, H.; Zhang, Y.; Li, M.; Wang, H.; Wang, D.; Wang, H.; Fu, Q.; Liu, M.; et al. A high-quality melon genome assembly provides insights into genetic basis of fruit trait improvement. *iScience* **2019**, *22*, 16–27. [CrossRef]
7. Yang, J.; Deng, G.; Lian, J.; Garraway, J.; Niu, Y.; Hu, Z.; Yu, J.; Zhang, M. The chromosome-scale genome of melon dissects genetic architecture of important agronomic traits. *iScience* **2020**, *23*, 101422. [CrossRef]
8. Périn, C.; Hagen, L.S.; de Conto, V.; Katzir, N.; Danin-Poleg, Y.; Portnoy, V.; Baudracco-Arnas, S.; Chadoeuf, J.; Dogimont, C.; Pitrat, M. A reference map of *Cucumis melo* based on two recombinant inbred line populations. *Theor. Appl. Genet.* **2002**, *104*, 1017–1034. [CrossRef]
9. Fukino, N.; Ohara, T.; Monforte, A.J.; Sugiyama, M.; Sakata, Y.; Kunihisa, M.; Matsumoto, S. Identification of QTLs for resistance to powdery mildew and SSR markers diagnostic for powdery mildew resistance genes in melon (*Cucumis melo* L.). *Theor. Appl. Genet.* **2008**, *118*, 165–175. [CrossRef]
10. Diaz, A.; Fergany, M.; Formisano, G.; Ziarsolo, P.; Blanca, J.; Fei, Z.; Staub, J.E.; Zalapa, J.E.; Cuevas, H.E.; Dace, G.; et al. A consensus linkage map for molecular markers and Quantitative Trait Loci associated with economically important traits in melon (*Cucumis melo* L.). *BMC Plant Biol.* **2011**, *11*, 111. [CrossRef]
11. Brotman, Y.; Kovalski, I.; Dogimont, C.; Pitrat, M.; Portnoy, V.; Katzir, N.; Perl-Treves, R. Molecular markers linked to papaya ring spot virus resistance and Fusarium race 2 resistance in melon. *Theor. Appl. Genet.* **2005**, *110*, 337–345. [CrossRef] [PubMed]
12. Brotman, Y.; Silberstein, L.; Kovalski, I.; Perin, C.; Dogimont, C.; Pitrat, M.; Klingler, J.; Thompson, G.A.; Perl-Treves, R. Resistance gene homologues in melon are linked to genetic loci conferring disease and pest resistance. *Theor. Appl. Genet.* **2002**, *104*, 1055–1063. [CrossRef] [PubMed]
13. Argyris, J.M.; Pujol, M.; Martín-Hernández, A.M.; Garcia-Mas, J. Combined use of genetic and genomics resources to understand virus resistance and fruit quality traits in melon. *Physiol. Plant.* **2015**, *155*, 4–11. [CrossRef]
14. Pereira, L.; Ruggieri, V.; Pérez, S.; Alexiou, K.G.; Fernández, M.; Jahrmann, T.; Pujol, M.; Garcia-Mas, J. QTL mapping of melon fruit quality traits using a high-density GBS-based genetic map. *BMC Plant Biol.* **2018**, *18*, 324. [CrossRef]
15. Argyris, J.M.; Díaz, A.; Ruggieri, V.; Fernández, M.; Jahrmann, T.; Gibon, Y.; Picó, B.; Martín-Hernández, A.M.; Monforte, A.J.; Garcia-Mas, J. QTL analyses in multiple populations employed for the fine mapping and identification of candidate genes at a locus affecting sugar accumulation in melon (*Cucumis melo* L.). *Front. Plant Sci.* **2017**, *8*, 1679. [CrossRef]
16. Wang, P.; Xu, X.; Zhao, G.; He, Y.; Hou, C.; Kong, W.; Zhang, J.; Liu, S.; Xu, Y.; Xu, Z. Genetic mapping and candidate gene analysis for melon resistance to *Phytophthora capsici*. *Sci. Rep.* **2020**, *10*, 20456. [CrossRef]
17. Giner, A.; Pascual, L.; Bourgeois, M.; Gyetvai, G.; Rios, P.; Picó, B.; Troadec, C.; Bendahmane, A.; Garcia-Mas, J.; Martín-Hernández, A.M. A mutation in the melon Vacuolar Protein Sorting 41 prevents systemic infection of *Cucumber mosaic virus*. *Sci. Rep.* **2017**, *7*, 10471. [CrossRef]
18. Brotman, Y.; Normantovich, M.; Goldenberg, Z.; Zvirin, Z.; Kovalski, I.; Stovbun, N.; Doniger, T.; Bolger, A.M.; Troadec, C.; Bendahmane, A.; et al. Dual resistance of melon to fusarium oxysporum races 0 and 2 and to papaya ring-spot virus is controlled by a pair of head-to-head-oriented nb-lrr genes of unusual architecture. *Mol. Plant* **2013**, *6*, 235–238. [CrossRef]
19. Shukla, D.D.; Ward, C.W.; Brunt, A.A. *The Potyviridae*; CAB International: Wallingford, UK, 1994.
20. Desbiez, C.; Lecoq, H. Zucchini yellow mosaic virus. *Plant Pathol.* **1997**, *46*, 809–829. [CrossRef]
21. Simmons, H.E.; Holmes, E.C.; Stephenson, A.G. Rapid evolutionary dynamics of zucchini yellow mosaic virus. *J. Gen. Virol.* **2008**, *89*, 1081–1085. [CrossRef]
22. Riechmann, J.L.; Lain, S.; Garcia, J.A. Highlights and prospects of potyvirus molecular biology. *J. Gen. Virol.* **1992**, *73*, 1–16. [CrossRef] [PubMed]
23. Urcuqui-Inchima, S.; Haenni, A.L.; Bernardi, F. Potyvirus proteins: A wealth of functions. *Virus Res.* **2001**, *74*, 157–175. [CrossRef]
24. Wang, D.; Li, G. Biological and molecular characterization of Zucchini yellow mosaic virus isolates infecting melon in Xinjiang, China. *Can. J. Plant Pathol.* **2017**, *39*, 48–59. [CrossRef]
25. Bubici, G.; Navarro, B.; Carluccio, A.V.; Ciuffo, M.; Di Serio, F.; Cillo, F. Genomic sequence variability of an Italian Zucchini yellow mosaic virus isolate. *Eur. J. Plant Pathol.* **2019**, *156*, 325–332. [CrossRef]

26. Chinnadurai, C.; Kollam, M.; Ramsubhag, A.; Jayaraman, J. Genome characterization of zucchini yellow mosaic virus infecting cucurbits reveals the presence of a new genotype in Trinidad and Tobago in the Caribbean region. *Arch. Virol.* **2021**, *166*, 1661–1669. [CrossRef]

27. Cordero, T.; Cerdan, L.; Carbonell, A.; Katsarou, K.; Kalantidis, K.; Daròs, J.A. Dicer-like 4 is involved in restricting the systemic movement of zucchini yellow mosaic virus in *Nicotiana benthamiana*. *Mol. Plant-Microbe Interact.* **2017**, *30*, 63–71. [CrossRef]

28. Revers, F.; García, J.A. Molecular biology of potyviruses. *Adv. Virus Res.* **2015**, *92*, 101–199. [CrossRef]

29. McCreight, J.D.; Bohn, G.W.; Kishaba, A.N. 'Pedigree' PI414723 melon. *Cucurbit. Genet. Coop. Rep.* **1992**, *15*, 51–52.

30. Pitrat, M.; Lecoq, H. Inheritance of zucchini yellow mosaic virus resistance in *Cucumis melo* L. *Euphytica* **1984**, *33*, 57–61. [CrossRef]

31. Fang, G.; Grumet, R. Genetic engineering of potyvirus resistance using constructs derived from the zucchini yellow mosaic virus coat protein gene. *Mol. Plant Microbe Interact.* **1993**, *6*, 358–367. [CrossRef]

32. Fuchs, M.; Gonsalves, D. Resistance of transgenic hybrid squash zw-20 expressing the coat protein genes of zucchini yellow mosaic virus and watermelon mosaic virus 2 to mixed infections by both potyviruses. *Bio/Tecnologye* **1995**, *13*, 1466–1473. [CrossRef]

33. Leibman, D.; Wolf, D.; Saharan, V.; Zelcer, A.; Arazi, T.; Yoel, S.; Gaba, V.; Gal-On, A. A high level of transgenic viral small RNA is associated with broad potyvirus resistance in cucurbits. *Mol. Plant-Microbe Interact.* **2011**, *24*, 1220–1238. [CrossRef] [PubMed]

34. Danin-Poleg, Y.; Tadmor, Y.; Tzuri, G.; Reis, N.; Hirschberg, J.; Katzir, N. Construction of a genetic map of melon with molecular markers and horticultural traits, and localization of genes associated with ZYMV resistance. *Euphytica* **2002**, *125*, 373–384. [CrossRef]

35. Harel-Beja, R.; Tzuri, G.; Portnoy, V.; Lotan-Pompan, M.; Lev, S.; Cohen, S.; Dai, N.; Yeselson, L.; Meir, A.; Libhaber, S.E.; et al. A genetic map of melon highly enriched with fruit quality QTLs and EST markers, including sugar and carotenoid metabolism genes. *Theor. Appl. Genet.* **2010**, *121*, 511–533. [CrossRef] [PubMed]

36. Galpaz, N.; Gonda, I.; Shem-Tov, D.; Barad, O.; Tzuri, G.; Lev, S.; Fei, Z.; Xu, Y.; Mao, L.; Jiao, C.; et al. Deciphering genetic factors that determine melon fruit-quality traits using RNA-Seq-based high-resolution QTL and eQTL mapping. *Plant J.* **2018**, *94*, 169–191. [CrossRef] [PubMed]

37. Herman, R.; Perl-Treves, R. Characterization and inheritance of a new source of resistance to *Fusarium oxysporum* f. sp. *melonis* race 1.2 in Cucumis melo. *Plant Dis.* **2007**, *91*, 1180–1186. [CrossRef]

38. Clark, M.F.; Adams, A.N. Characteristics of the microplate method of enzyme linked immunosorbent assay for the detection of plant viruses. *J. Gen. Virol.* **1977**, *34*, 475–483. [CrossRef]

39. Luo, M.; Wang, Y.H.; Frisch, D.; Joobeur, T.; Wing, R.A.; Dean, R.A. Melon bacterial artificial chromosome (BAC) library construction using improved methods and identification of clones linked to the locus conferring resistance to melon Fusarium wilt (*Fom-2*). *Genome* **2001**, *44*, 154–162. [CrossRef]

40. Bohn, G.W.; Kishaba, A.N.; McCreight, J.D. WMR-29 muskmelon breeding line. *HortScience* **1980**, *15*, 539–540.

41. Budiman, M.A.; Mao, L.; Wood, T.C.; Wing, R.A. A deep-coverage tomato BAC library and prospects toward development of an STC framework for genome sequencing. *Genome Res.* **2000**, *10*, 129–136. [CrossRef]

42. Neff, M.M.; Turk, E.; Kalishman, M. Web-based primer design for single nucleotide polymorphism analysis. *Trends Genet.* **2002**, *18*, 613–615. [CrossRef]

43. Sonnhammer, E.L.L.; Eddy, S.R.; Birney, E.; Bateman, A.; Durbin, R. Pfam: Multiple sequence alignments and HMM-profiles of protein domains. *Nucleic Acids Res.* **1998**, *26*, 320–322. [CrossRef]

44. Kurtz, S.; Phillippy, A.; Delcher, A.L.; Smoot, M.; Shumway, M.; Antonescu, C.; Salzberg, S.L. Versatile and open software for comparing large genomes. *Genome Biol.* **2004**, *5*, R12. [CrossRef] [PubMed]

45. Slater, G.S.C.; Birney, E. Automated generation of heuristics for biological sequence comparison. *BMC Bioinform.* **2005**, *6*, 31. [CrossRef] [PubMed]

46. Silberstein, L.; Kovalski, I.; Brotman, Y.; Perin, C.; Dogimont, C.; Pitrat, M.; Klingler, J.; Thompson, G.; Portnoy, V.; Katzir, N.; et al. Linkage map of *Cucumis melo* including phenotypic traits and sequence-characterized genes. *Genome* **2003**, *46*, 761–773. [CrossRef] [PubMed]

47. Robinson, J.T.; Thorvaldsdóttir, H.; Winckler, W.; Guttman, M.; Lander, E.S.; Getz, G.; Mesirov, J.P. Integrative Genome Viewer. *Nat. Biotechnol.* **2011**, *29*, 24–26. [CrossRef] [PubMed]

48. Meyers, B.C.; Kozik, A.; Griego, A.; Kuang, H.; Michelmore, R.W. Genome-wide analysis of NBS-LRR-encoding genes in Arabidopsis. *Plant Cell* **2003**, *15*, 809–834. [CrossRef] [PubMed]

49. Huang, S.; Li, R.; Zhang, Z.; Li, L.; Gu, X.; Fan, W.; Lucas, W.J.; Wang, X.; Xie, B.; Ni, P.; et al. The genome of the cucumber, *Cucumis sativus* L. *Nat. Genet.* **2009**, *41*, 1275–1281. [CrossRef]

50. Kapos, P.; Devendrakumar, K.T.; Li, X. Plant NLRs: From discovery to application. *Plant Sci.* **2019**, *279*, 3–18. [CrossRef]

51. Dogimont, C.; Chovelon, V.; Pauquet, J.; Boualem, A.; Bendahmane, A. The *Vat* locus encodes for a CC-NBS-LRR protein that confers resistance to *Aphis gossypii* infestation and *A. gossypii*-mediated virus resistance. *Plant J.* **2014**, *80*, 993–1004. [CrossRef]

52. Joobeur, T.; King, J.J.; Nolin, S.J.; Thomas, C.E.; Dean, R.A. The fusarium wilt resistance locus *Fom-2* of melon contains a single resistance gene with complex features. *Plant J.* **2004**, *39*, 283–297. [CrossRef]

53. Nieto, C.; Morales, M.; Orjeda, G.; Clepet, C.; Monfort, A.; Sturbois, B.; Puigdomènech, P.; Pitrat, M.; Caboche, M.; Dogimont, C.; et al. An eIF4E allele confers resistance to an uncapped and non-polyadenylated RNA virus in melon. *Plant J.* **2006**, *48*, 452–462. [CrossRef]

54. Taler, D.; Galperin, M.; Benjamin, I.; Cohen, Y.; Kenigsbuch, D. Plant eR genes that encode photorespiratory enzymes confer resistance against disease. *Plant Cell* **2004**, *16*, 172–184. [CrossRef] [PubMed]

55. Danin-Poleg, Y.; Paris, H.S.; Cohen, S.; Rabinowitch, H.D.; Karchi, Z. Oligogenic inheritance of resistance to zucchini yellow mosaic virus in melons. *Euphytica* **1997**, *93*, 331–337. [CrossRef]

56. Goldenberg, T. High Resolution Mapping and Physical Delimitation of the *Fom-1/Prv* and *Zym* Loci in Melon. Ph.D. Thesis, Bar Ilan University, Ramat Gan, Israel, 2009.

57. Díaz, J.A.; Mallor, C.; Carmen Soria, C.; Rocío Camero, R.; Elisa Garzo, E.; Alberto Fereres, A.; Alvarez, J.M.; Gómez-Guillamón, M.L.; Luis-Arteaga, E.M. Potential sources of resistance for melon to nonpersistently aphid-borne viruses. *Plant Dis.* **2003**, *87*, 960–964. [CrossRef] [PubMed]

58. Romay, G.; Pitrat, M.; Lecoq, H.; Wipf-Scheibel, C.; Millot, P.; Girardot, G.; Desbiez, C. Resistance against melon chlorotic mosaic virus and tomato leaf curl New Delhi virus in melon. *Plant Dis.* **2019**, *103*, 2913–2919. [CrossRef] [PubMed]

59. van Wersch, R.; Li, X.; Zhang, Y. Mighty dwarfs: Arabidopsis autoimmune mutants and their usages in genetic dissection of plant immunity. *Front. Plant Sci.* **2016**, *7*, 1717. [CrossRef] [PubMed]

60. Venkatesh, J.; Kang, B.C. Current views on temperature-modulated R gene-mediated plant defense responses and tradeoffs between plant growth and immunity. *Curr. Opin. Plant Biol.* **2019**, *50*, 9–17. [CrossRef]

61. Olsen, A.N.; Ernst, H.A.; Leggio, L.L.; Skriver, K. Transcriptional networks in plants NAC transcription factors: Structurally distinct, functionally diverse. *Trends Plant Sci.* **2005**, *10*, 79–87. [CrossRef] [PubMed]

62. Singh, S.; Koyama, H.; Bhati, K.K.; Alok, A. The biotechnological importance of the plant-specific NAC transcription factor family in crop improvement. *J. Plant Res.* **2021**, *134*, 475–495. [CrossRef]

63. Wang, X.; Goregaoker, S.P.; Culver, J.N. Interaction of the tobacco mosaic virus replicase protein with a NAC domain transcription factor is associated with the suppression of systemic host defenses. *J. Virol.* **2009**, *83*, 9720–9730. [CrossRef] [PubMed]

64. Xie, Q.; Sanz-Burgos, A.P.; Guo, H.; García, J.A.; Gutiérrez, C. GRAB proteins, novel members of the NAC domain family, isolated by their interaction with a geminivirus protein. *Plant Mol. Biol.* **1999**, *39*, 647–656. [CrossRef] [PubMed]

65. Selth, L.A.; Dogra, S.C.; Rasheed, M.S.; Healy, H.; Randles, J.W.; Rezaian, M.A. A NAC domain protein interacts with Tomato leaf curl virus replication accessory protein and enhances viral replication. *Plant Cell* **2005**, *17*, 311–325. [CrossRef]

66. Bergelson, J.; Kreitman, M.; Stahl, E.A.; Tian, D. Evolutionary dynamics of plant R-genes. *Science* **2001**, *292*, 2281–2285. [CrossRef] [PubMed]

67. Friedman, A.R.; Baker, B.J. The evolution of resistance genes in multi-protein plant resistance systems. *Curr. Opin. Genet. Dev.* **2007**, *17*, 493–499. [CrossRef] [PubMed]

68. Kabelka, E.; Ullah, Z.; Grumet, R. Multiple alleles for zucchini yellow mosaic virus resistance at the *zym* locus in cucumber. *Theor. Appl. Genet.* **1997**, *95*, 997–1004. [CrossRef]

69. Amano, M.; Mochizuki, A.; Kawagoe, Y.; Iwahori, K.; Niwa, K.; Svoboda, J.; Maeda, T.; Imura, Y. High-resolution mapping of *zym*, a recessive gene for Zucchini yellow mosaic virus resistance in cucumber. *Theor. Appl. Genet.* **2013**, *126*, 2983–2993. [CrossRef] [PubMed]

70. Pascual, L.; Yan, J.; Pujol, M.; Monforte, A.J.; Picó, B.; Martín-Hernández, A.M. CmVPS41 is a general gatekeeper for resistance to cucumber mosaic virus phloem entry in melon. *Front. Plant Sci.* **2019**, *10*, 1219. [CrossRef]

71. García-Almodóvar, R.C.; Gosalvez, B.; Aranda, M.A.; Burgos, L. Production of transgenic diploid *Cucumis melo* plants. *Plant Cell. Tissue Organ Cult.* **2017**, *130*, 323–333. [CrossRef]

72. Chovelon, V.; Restier, V.; Giovinazzo, N.; Dogimont, C.; Aarrouf, J. Histological study of organogenesis in *Cucumis melo* L. after genetic transformation: Why is it difficult to obtain transgenic plants? *Plant Cell Rep.* **2011**, *30*, 2001–2011. [CrossRef]